

## Acrylic/casein latexes with controlled degree of grafting and improved coating performance

Matías L. Picchio <sup>a,b</sup>, Mario C.G. Passeggi Jr. <sup>c,d</sup>, María J. Barandiaran <sup>e</sup>, Luis M. Gugliotta <sup>a,d</sup>, Roque J. Minari <sup>a,d,\*</sup>

<sup>a</sup> Group of Polymers and Polymerization Reactors, INTEC (Universidad Nacional del Litoral-CONICET), Güemes 3450, Santa Fe 3000, Argentina

<sup>b</sup> Facultad Regional Villa María (Universidad Tecnológica Nacional), Av. Universidad 450, Villa María 5900, Argentina

<sup>c</sup> Physics of Surfaces and Interfaces Laboratory, IFIS Litoral (Universidad Nacional del Litoral-CONICET), Güemes 3450, Santa Fe 3000, Argentina

<sup>d</sup> Facultad de Ingeniería Química (Universidad Nacional del Litoral), Santiago del Estero 2829, Santa Fe 3000, Argentina

<sup>e</sup> POLYMAT and Departamento de Química Aplicada, University of the Basque Country UPV/EHU, Centro Joxe Mari Korta, Avenida Tolosa 72, 20018, Donostia-San Sebastián, Spain



### ARTICLE INFO

#### Article history:

Received 22 February 2016

Received in revised form

27 September 2016

Accepted 3 October 2016

#### Keywords:

Bio-based materials

Acrylic/casein hybrid nanocomposites

Controlled degree of grafting

Waterborne coatings

### ABSTRACT

The production of acrylic/casein nanocomposites constitutes a promising alternative for developing new materials from renewable resources and with an important substitution of petroleum based monomers. Unfortunately, a low degree of grafting between both components limits their successful application in many fields. This proposal opens the opportunity for synthesizing polymer/casein nanocomposites with controlled degree of grafting by using, in the emulsifier-free emulsion polymerization of acrylic monomers, highly-methacrylated casein with varied degree of functionalization. The benefits of this strategy are assessed by analyzing the performance of the obtained hybrid nanocomposites for their application as bio-based waterborne coatings.

© 2016 Elsevier B.V. All rights reserved.

## 1. Introduction

There is an urgent need to develop polymeric materials from renewable resources due to the fast depletion and dramatic price fluctuations of fossil oils, and the increasingly consumers preference toward bio-based products [1–3]. Among the different bio-based resources, natural proteins constitute a promising candidate as they contain amine and carboxyl functionalities that present unlimited opportunities to introduce modification in their structure [4]. Indeed, casein from bovine milk has been used for a long time as a film-forming material in many industrial applications [5,6]. However, the casein films present low resistance to water immersion, susceptibility to microbial attack, and poor mechanical properties [7]. For these reasons, the incorporation of synthetic polymers, such as acrylates, has gained technological interest because it attempts to modify and improve the properties of pure casein [8].

Emulsion polymerization of acrylic monomers in the presence of casein has been previously studied using thermal and redox initiators in absence of emulsifier [9–16]. However, in such works very few efforts have been made to characterize the molecular microstructure of the hybrid polymer. Li et al. [17,18] also reported the synthesis of poly(methyl methacrylate)(PMMA)/casein latexes via emulsifier-free emulsion polymerization. Grafting of casein with PMMA was conducted, by initiating the polymerization according to a redox reaction between an alkyl hydroperoxide and the amine groups of the casein. Then, the propagation of amine casein radicals initiated the graft polymerization and the formation of compatibilized nanoparticles. Following the Li et al. proposal, the grafting degree of casein along the MMA emulsion polymerization performed in the presence of varied protein concentration was quantified, observing that as the concentration of casein increased, the fraction of grafted protein decreased [19]. In other words, the use of high casein concentrations, which is highly desirable for a better exploitation of this renewable resource, limited the fraction of grafted acrylic/casein copolymer.

Recently, the film performance of acrylic/casein latexes in waterborne coatings was evaluated [20], finding that hybrid materials present promising properties. Unfortunately, films showed a poor resistance to water, as a consequence of the high amount

\* Corresponding author at: Group of Polymers and Polymerization Reactors, INTEC (Universidad Nacional del Litoral-CONICET), Güemes 3450, Santa Fe 3000, Argentina.

E-mail address: [rjminari@santafe-conicet.gov.ar](mailto:rjminari@santafe-conicet.gov.ar) (R.J. Minari).

of ungrafted casein in the hybrid latexes. The low degree of acrylic/casein grafting reached during the synthesis of these hybrid materials is the main drawback for their successful application.

A previously explored alternative to promote acrylic grafting onto casein chains is the protein chemical modification with acrylic acid (AA) and 1-ethyl-3-(3-dimethylaminopropyl)carbodiimide (EDC) as activator [21]. The main disadvantages of this approach are: (i) the low casein acylation, restricted by the AA concentration used during the protein modification, because the presence of AA could lead to protein coagulation (pH of casein isoelectric point = 4.0); and (ii) the high cost of EDC that limits the large-scale implementation. This approach improved the fraction of protein grafted, but the increment of compatibility degree, restricted by casein acylation, was not enough to fulfill the requirements of an industrial film-forming application. Due to casein is a large protein, with an average molecular weight of 30000 g/mol, a superior number of grafting points are needed to obtain a material highly compatibilized.

This work proposes, as a strategy to overcome the previously found limitations in lowly compatibilized hybrid systems, the use of highly-methacrylated caseins (MC) together with the formation of free radicals onto protein chains by redox initiation in an emulsifier-free emulsion polymerization. The chemical modification of casein, based on an amine-glycidyl ether reaction, allows appropriately controlling the protein grafting of the hybrid nanoparticles by varying the protein methacrylation degree. The improved compatibility obtained by the proposed strategy was evaluated in a coating application by measuring sensitive properties of the hybrid films.

## 2. Experimental

### 2.1. Materials

Technical grade casein from bovine milk (Sigma), methyl methacrylate (MMA), butyl acrylate (BA) and glycidyl methacrylate (GMA) (Aldrich) were used as supplied. The employed initiator was *tert*-butyl hydroperoxide (TBHP, Aldrich). Other used reagents were: tetrahydrofuran (THF, Cicarelli), sodium carbonate ( $\text{Na}_2\text{CO}_3$ , Cicarelli) as buffer to regulate the pH, absolute ethanol (Cicarelli), sodium borate (Anedra), 2-mercaptoethanol (Fluka), sodium dodecyl sulphate (SDS, Anedra), glycine amino-acid (Sigma) and methyl ethyl ketone (MEK, Anedra). O-phthalaldehyde (OPA, Sigma) was used as fluorescent amino marker. Uranyl acetate 1 wt% solution (UAc, EMS) and formvar® (polyvinyl formal, Fluka) were used for TEM sample preparation. All the reagents were used as received without any kind of purification. Distilled and deionized water was used throughout the work.

### 2.2. Synthesis of acrylic/casein hybrid latexes with high degree of compatibility

Hybrid latexes with high compatibility were produced by surfactant-free emulsion polymerization, using highly methacrylated casein together with BA/MMA as main monomers, and TBHP as initiator.

The methacrylated casein was synthesized by the amine-glycidyl ether reaction [22]. For this purpose, casein was first dissolved at 50 °C in a water solution containing 0.4% wt/wt of  $\text{Na}_2\text{CO}_3$  to regulate the pH. The reaction solution pH was higher than 10, where the association of casein macromolecules by hydrophobic interaction is reduced [23]. Then, GMA was loaded and the reaction was run for 4 h. Samples were taken at the beginning and at the end of reaction, and then analyzed by  $^1\text{H}$  NMR.

**Table 1**

Formulation for the synthesis of acrylic/casein latexes.

Reagent	Amounts [pphm*]
BA	80
MMA	20
Neat/Methacrylated Casein <sup>#</sup>	25
TBHP	0.2
$\text{Na}_2\text{CO}_3$	2.5
$\text{H}_2\text{O}$	500

\*pphm: part per hundred monomer. <sup>#</sup> in all cases the neat amount of casein is 25 pphm, therefore for Methacrylated Casein additional amounts are considered as result of the GMA incorporation during the functionalization reaction.

The methacrylation reaction of casein proceeds by nucleophilic attack of their amine groups on the least substituted carbon of the oxirane group of GMA, producing the ring opening and the subsequent formation of an amine with a methacrylic group [24]. Thus, the synthesized MC presents a new methacrylic functionality, which together with the remainder amine groups, has the capacity to radically propagate during the polymerization.

Different molar ratios GMA/casein (2, 10, 20 and 40) were employed, assuming 30000 g/mol as the average molecular weight of casein, and taking into consideration that the amine groups per casein molecule available to react with oxiranes are 40 primary amines (on average) and a higher amount of secondary ones. Notice that methacrylation was carried out in aqueous media, which represents an important advantage due to the resulting MC solution can be directly used in the polymerization reaction.

After obtaining MC, the solution temperature was raised up to 80 °C and the (meth)acrylic monomers were loaded. The resulting dispersion was purged with  $\text{N}_2$  for 30 min and then the TBHP was injected in order to redox initiate the polymerization with the available casein amine groups, producing amine and terbutoxy radicals. By propagation through the primary amine radical, casein grafted onto the polymer backbone is formed. On the other hand, terbutoxy radicals can propagate with the (meth)acrylic monomers producing (meth)acrylate polymer, as well as with the pendant methacrylic groups onto casein chain, forming grafted casein. Fig. 1 schematizes the employed strategy. The involved mechanisms in the production and growth of acrylic/casein hybrid nanoparticles are described in detail elsewhere [16].

Table 1 summarizes the formulation of the performed emulsion polymerizations of acrylic monomers in the presence of 25 pphm of casein (native and MC). This formulation was used aiming at obtaining a copolymer with a glass transition temperature ( $T_g$ ) suitable to be used as coating. In fact, BA/MMA (50/50) is usually used in conventional coating formulations. In this work, the hard MMA was partially substituted by the high  $T_g$  bio-based modified casein. The whole process (MC synthesis and emulsion polymerization) was performed in a 0.5 L jacketed reactor equipped with thermostatic bath, thermometer, condenser, stirrer,  $\text{N}_2$  inlet and sampling device. In the case of the latex synthesized with native casein, it was previously dissolved at 50 °C, before polymerization.

### 2.3. Characterization of the methacrylated casein and latexes

Casein methacrylation was evaluated by (i)  $^1\text{H}$  NMR spectroscopy; and (ii) quantifying the effective percentage of GMA bounded to casein with the OPA method [25,26]. The  $^1\text{H}$  NMR spectra were obtained with a Bruker Advance II 300 spectrometer, using the WATERGATE sequence to suppress the signal of water. The OPA method consists in the reaction of this reagent with primary amine groups of proteins to form highly fluorescent 1-alkylthio-2-alkyl substituted isoindoles, which show an absorption band at 340 nm [27]. The percentage of GMA bounded per casein molecule was determined on the basis of the consumption of casein amine

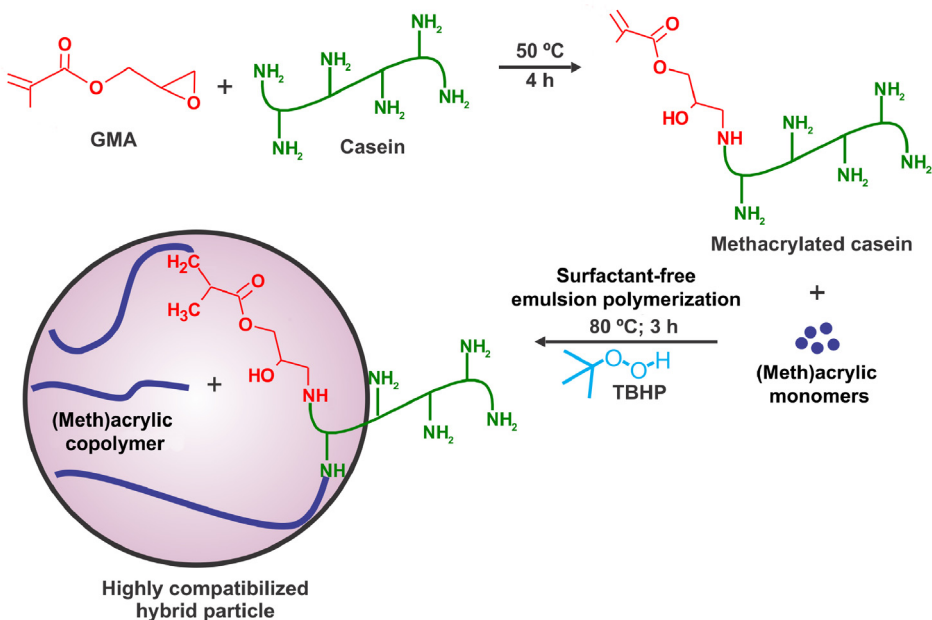


**Fig. 1.** Scheme of the synthesis strategy for producing highly compatibilized hybrid latexes.

groups during the methacrylation reaction. Therefore, the amine groups concentration was calculated by measuring the absorbance at 340 nm of MC against that of native casein and employing a calibration, that relates the absorbance with the amine concentration, obtained with glycine as standard. The overall monomer conversion ( $x$ ) was determined gravimetrically and casein was not considered in the  $x$  calculation. Average particle diameters ( $d_p$ ) were measured at 30 °C by dynamic light scattering, using a Brookhaven BI-9000 AT photometer at a detection angle of 90°.

The degree of compatibility of the hybrid latexes was mainly determined by measuring the fraction of casein grafted to the acrylic polymer (casein grafting efficiency, CGE). CGE was determined following a procedure previously reported [19]. Also, the insoluble fraction (IF) of the hybrid materials was quantified by comparing the dried weights of the sample before and after the soxhlet extraction with THF for 24 h. Notice that the insoluble fraction is composed by the acrylic gel, the free casein (which is also insoluble in THF) and the acrylic-graft-casein copolymer.

Furthermore, compatibility of latex particles was evaluated by transmission electron microscopy (TEM), using a TECNAI G2 20TWIN (200 kV, LaB6). A drop of diluted latex (0.01 wt% of solids content) was dried on a formvar coated copper grid. Then, a drop of 1 wt% UAc solution was added to negatively stain the surface particles and solid objects [28].

#### 2.4. Characterization of the hybrid materials

Films with a final thickness of about 1 mm were prepared by casting the dispersions onto silicone molds and then they were dried at 22 °C and 55% relative humidity during 7 days.

The film morphology of the hybrid nanocomposites was determined by Atomic Force Microscopy (AFM) using a commercial Nanotec Electronic equipment operating in tapping and jumping modes. For surface imaging, latexes were cast onto seal paper using a 120 µm wet-thickness frame applicator and drying at room temperature for 24 h. For cross-section AFM imaging, films with a thickness of about 1 mm were cut using a cryogenically cooled microtome (Leica EM UC6) under liquid nitrogen. Silicon cantilevers (All-In-One, Budget Sensors, Bulgaria) with a nominal spring constant of  $k = 40 \text{ N/m}$  and resonance frequency of 350 kHz

were used for tapping mode, while for jumping mode those parameters were 2.7 N/m and 80 kHz, respectively. AFM experiments were performed in air at room temperature. Acquisition and image processing were performed using the WS × M free software [29]. AFM Jumping mode was used to generate stiffness maps with a grid of 256 points × 256 points on a 3 µm × 3 µm area of the sample.

Thermal stability of the nanocomposites was studied by thermogravimetric analysis (TGA). To this effect, samples of 10 mg were heated from 40 to 600 °C with a heating rate of 10 °C/min under nitrogen atmosphere using a Mettler-Toledo Thermogravimetric Analyzer, model TG-50. The maximal decomposition temperature ( $T_{d,max}$ ) was determined as the temperature at main peak of the derivative weight loss curve.

Contact angles (CA) of water on the film surfaces were measured by employing a homemade goniometer. To this effect a 120 µm film was cast on a glass plate and distilled water droplets of 30 µL were deposited onto the surface of the film. The average contact angle data were obtained from twenty measurements of each sample.

Face-to-face blocking resistance of the films was evaluated according to ASTM D 4946-89 and following a procedure described elsewhere [20]. The test for each sample was run three times and the results were correlated to rates 0–10 (minimum and maximum blocking resistance, respectively) defined by ASTM D 4946-89.

The open time of the latexes was evaluated by the optical technique so called Adaptive Speckle Imaging Interferometry (ASII) in the Horus equipment (Formulaction). For the analysis, films were cast on a glass (90 µm wet) and the drying kinetics was studied over 2.4 h.

Tensile tests of films with dumbbell shape of length 9.53 mm and cross section  $3.18 \times 1 \text{ mm}^2$  were carried out with an elongation rate of 25 mm/min. Film hardness was correlated with the maximum value of the force measured in compression when the sample is penetrated 1 mm with a 4 mm cylinder plane-probe. Both analysis were carried out in a universal testing machine (INSTRON 3344), at 23 °C and 50% relative humidity and at least five specimens of each sample were tested.

For water and organic solvent resistance analysis, film specimens of 1 mm of thickness and 20 mm in diameter were immersed in distilled water and MEK at room temperature. Specimens were removed from the solvent (water or MEK) at a regular time,

dried with a filter paper, and immediately weighed before being immersed. This procedure was repeated during 7 days, measuring the relative mass absorbed ( $A_W$  and  $A_{MEK}$ ) and the weight loss ( $WL_W$  and  $WL_{MEK}$ ), expressed as the percentage of the dissolved mass of the dried film.

The effect of the compatibility increase on the biodegradation ability of hybrid films was qualitatively evaluated by soil burial degradation experiments. For this purpose, film samples of 20 mm in diameter were buried in a moisturized commercial compost with the following characteristics: total dry solid = 45% of the wet solids; pH = 6.5; and non volatile-solids content = 40% of the wet solids. Before using the compost, it was screened by a 3 1/2 mesh sieve. During the test the relative humidity and temperature of the compost were controlled at 55% and 30 °C, respectively. The samples were removed every 7 days, carefully cleaned for ensuring the stop of the degradation and then dried in oven at 60 °C up to a constant weight. Finally, biodegradation was determined as the weight loss ( $W_{loss}$ ) of the film samples.

The effect of biodegradation on the surface morphology of the biodegraded films was examined by Scanning Electron Microscopy (SEM) using a Zeiss Sigma equipment. For SEM analysis, biodegraded films were coated with gold in a sputter coater and observed under SEM at an accelerating voltage of 2.0 kV.

### 3. Results and discussion

#### 3.1. Synthesis of the methacrylated casein (MC)

**Fig. 2** presents the characterization by  $^1\text{H}$  NMR of casein methacrylation for a GMA/casein molar ratio of 20. **Fig. 2a** shows the  $^1\text{H}$  NMR spectrum of GMA and its main characteristic peaks. The methyl protons of the GMA are located at 1.9 ppm, the oxirane protons at 2.6, 2.8 and 3.2 ppm, the methylene protons at 3.9 and 4.5 ppm, and the methacrylic protons at 5.7 and 6.1 ppm. The  $^1\text{H}$  NMR spectrum of native casein between 2.5 and 3.5 ppm is showed in **Fig. 2b**. Comparison of the  $^1\text{H}$  NMR spectra of the mixture GMA and casein, acquired before and after the methacrylation reaction (**Figs. 2c** and **d**) shows that: (i) the peaks of methacrylic protons of the GMA (f,g) remained unaffected after MC synthesis; while (ii) the peaks of oxirane protons of GMA (c,d,e) were considerable reduced. It is an indication that the MC was satisfactorily synthesized. The percentage of GMA bounded to casein, was evaluated by the OPA method, resulting 100%, 87% and 79% for GMA/casein molar ratios of 2, 20 and 40, respectively. In this way, the maximum functionality reached was 32 vinyl double bonds per molecule of casein.

#### 3.2. Synthesis of the acrylic/casein hybrid latexes

Herein, the results of the emulsifier-free emulsion polymerization of BA/MMA are presented with a monomer ratio of 80/20 and in the presence of native and functionalized casein with different degree of methacrylation. The experiment codes contain the abbreviation MC with a subscript that indicates the theoretical amount of methacrylic groups incorporated to casein. Thus, in the experiment MC<sub>20</sub> casein with a molar ratio methacrylic groups/protein molecule of 20 was used in the latex synthesis; while MC<sub>0</sub> correspond to the latex prepared with native casein. **Table 2** summarizes the final values  $x$ ,  $d_p$ , number of particles per liter of latex (Np), CGE, and IF, whereas **Fig. 3a** and **b** shows the evolution along the polymerizations of  $x$  and CGE.

It must be noted that the increment of the degree of casein methacrylation from 2 up to 40, decreased both the polymerization rate and the final  $x$ . According to Li et al. [17], this behavior is expected because the reaction is started by interaction of the

**Table 2**

Main results of BA/MMA emulsion polymerization in the presence of native and methacrylated casein.

Experiment	$x$ (%)	$d_p$ (nm)	Np (#/L)	CGE (%)	IF (%)
MC <sub>0</sub>	91	122	$1.42 \times 10^{17}$	20	85
MC <sub>2</sub>	90	155	$6.82 \times 10^{16}$	25	96
MC <sub>10</sub>	82	172	$4.71 \times 10^{16}$	34	98
MC <sub>20</sub>	80	186	$3.54 \times 10^{16}$	59	98
MC <sub>40</sub>	74	207	$2.37 \times 10^{16}$	76	99

hydroperoxide molecules with the remainder amine groups of casein. It is worth to remark that initiation by thermal dissociation is neglected at the employed conditions [ $k_d(\text{TBHP}) \sim 10^{-10} \text{ s}^{-1}$  at 80 °C], and for this reason initiation is limited to the reaction of TBHP with amine groups. Then, the incorporation of methacrylic groups onto casein chains appreciably reduced the quantity of amine groups (**Fig. 1**), affecting its availability for initiating the polymerization with TBHP and probably the emulsifier ability of the protein. Thus, the radical concentration and the number of nucleated polymer particles were decreased (in **Table 2** Np varied from  $1.42 \times 10^{17}$  for native casein, down to  $2.37 \times 10^{16}$  for MC<sub>40</sub>).

On the other hand, the most important improvement obtained by protein modification was the increment in the degree of compatibility of acrylic/casein latexes, which is observed by the significant increase of CGE with respect to the native casein. The increment in the methacrylation degree of MC allowed the adequate control of the fraction of grafted casein, which varied from 20% (for MC<sub>0</sub>) to 76% (for MC<sub>40</sub>), and the amount of grafted acrylic chains on the protein backbone. It represents a significant enhancement, where the mass of linked biomaterial was augmented by more than 270% with respect to the unmodified protein. Meanwhile, IF was also increased with the number of double bonds incorporated onto casein, namely a higher fraction of grafted acrylic was obtained. Furthermore, based on the number of double bonds present in the protein, it would be expected that these higher levels of IF correlate with the existence of cross-linked structures in the material.

These results suggest that the high values of CGE and IF reached with MC are sufficient to guarantee that almost all of the nanoparticles are compatibilized. It means that latexes are more homogeneous when MC is used, in the sense of the fraction of ungrafted casein and acrylic polymer is significantly reduced.

**Fig. 3b** presents the evolution of CGE measured during the polymerizations. Notice that with MC, the grafting did not remain constant as in the case with native casein [19]. When MC was employed, CGE increased until  $x$  reached 55–60%, indicating that incorporation of MC was more important in the first half part of reaction. Despite CGE remains unmodified beyond  $x = 60$ , propagation of pendant methacrylic groups of MC could continue increasing the fraction of grafted acrylic (a high IF of 99% was reached). When highly methacrylated casein was used (i.e., latexes MC<sub>10</sub>, MC<sub>20</sub>, and MC<sub>40</sub>) a significant amount of grafting points per protein was reached.

**Fig. 4** shows the TEM micrographs of nanoparticles obtained from latexes MC<sub>0</sub> (native casein) and MC<sub>40</sub>, prepared with the same dilution. It can be observed that the sample synthesized with native casein presents many dark regions, which corresponds to the ungrafted protein stained with UAc (**Fig. 4a**). However, when using MC<sub>40</sub> (**Fig. 4b**), the amount of free casein observed in the latex was significantly reduced, indicating a higher compatibility and a strong attachment between casein and acrylic polymer. This observation is in agreement with the higher CGE reached with MC<sub>40</sub>.

#### 3.3. Morphology of the hybrid materials

**Fig. 5a–d** shows AFM phase images of the films surface synthesized with different MC. The internal morphologies of the materials

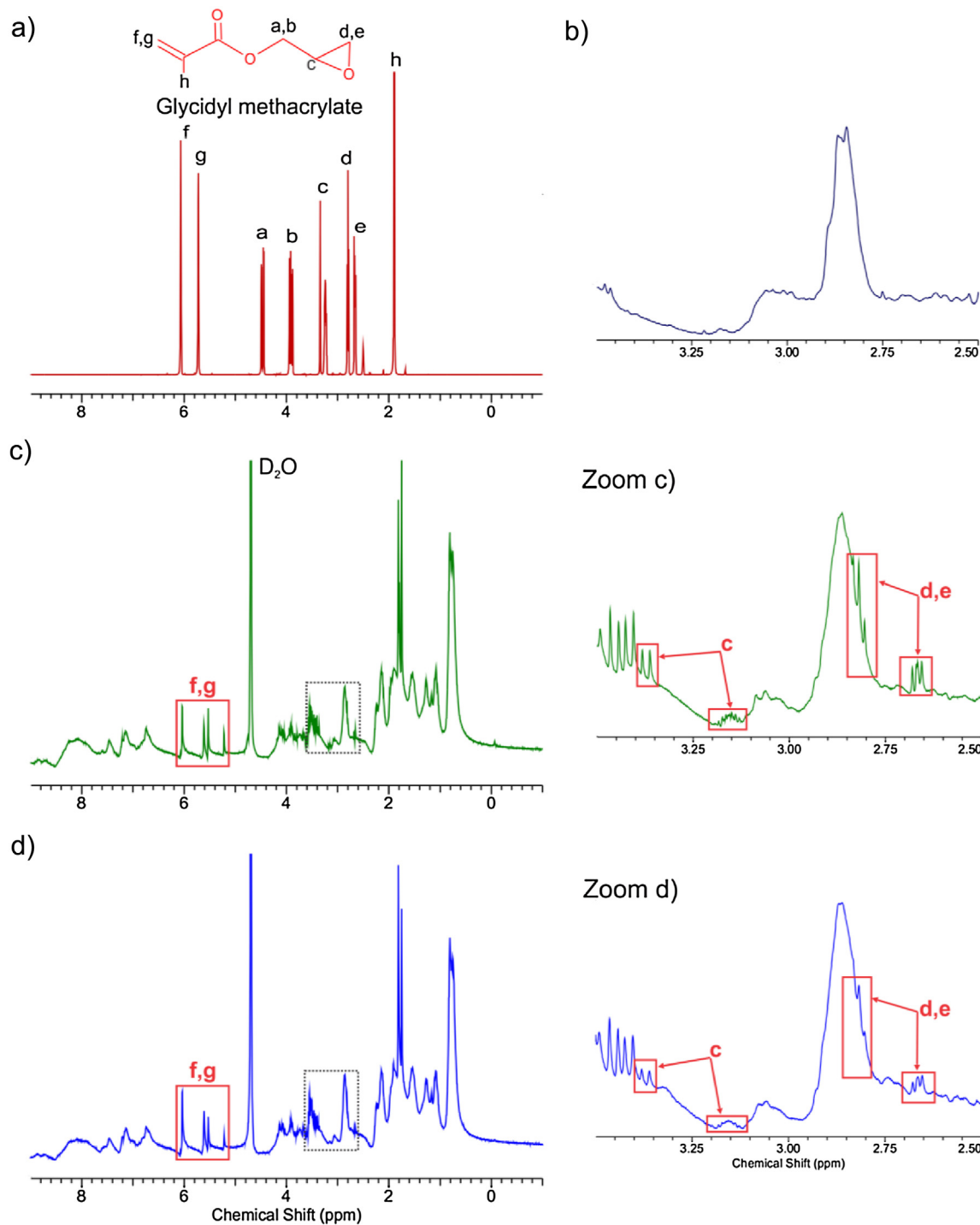


**Fig. 2.** <sup>1</sup>H NMR spectra of (a) GMA, (b) native casein between 2.5 and 3.5 ppm, and (c) GMA-casein mixture before and (d) after the methacrylation reaction for a GMA/casein molar ratio of 20.

MC<sub>0</sub> and MC<sub>40</sub> are also shown in the stiffness images of Fig. 6a and b. In such images (phase or stiffness), the soft domains corresponding to the acrylic polymer are shown in dark color, while hard domains of casein are in light color.

Notice that, with native casein (MC<sub>0</sub>, Fig. 5a), the film surface is mainly composed by soft acrylic polymer with some hard domains of casein. Also, the cross-section of MC<sub>0</sub> film (Fig. 6a) shows a high proportion of rigid casein in relation to the acrylic domains, exhibiting phase migration and a limited compatibility between the components. As it was earlier mentioned, a large amount of

non-linked casein, which remains solubilized in water, is present in the MC<sub>0</sub> latex. In this scenery, ungrafted casein can migrate inside the film, while the top film surface became enriched with soft hydrophobic acrylic particles [30]. This vertical components stratification is attributed to diffusional effects. During film formation, a rapid casein diffusion in relation to water evaporation is expected due to the high molecular mobility of this protein. Thus, a uniform vertical profile is predicted because the dissolved free casein goes down in the film as the waterfront decreases, leading to a film surface composed mainly by acrylic polymer with

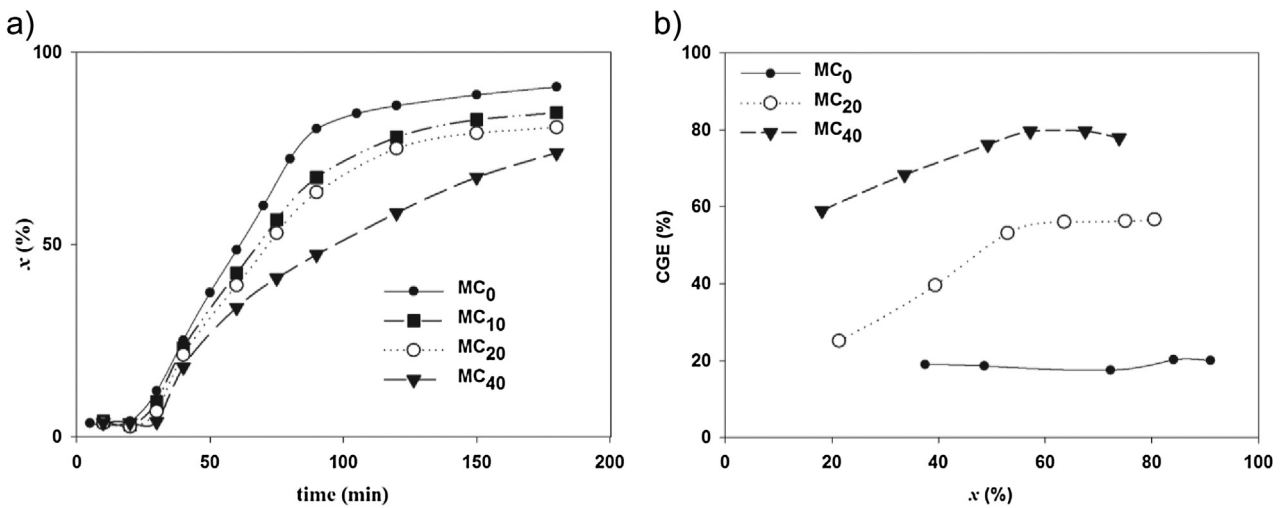


**Fig. 3.** BA/MMA emulsion polymerization in the presence of native and functionalized casein with different degree of methacrylation. Evolution of: (a) monomer conversion, and (b) CGE.

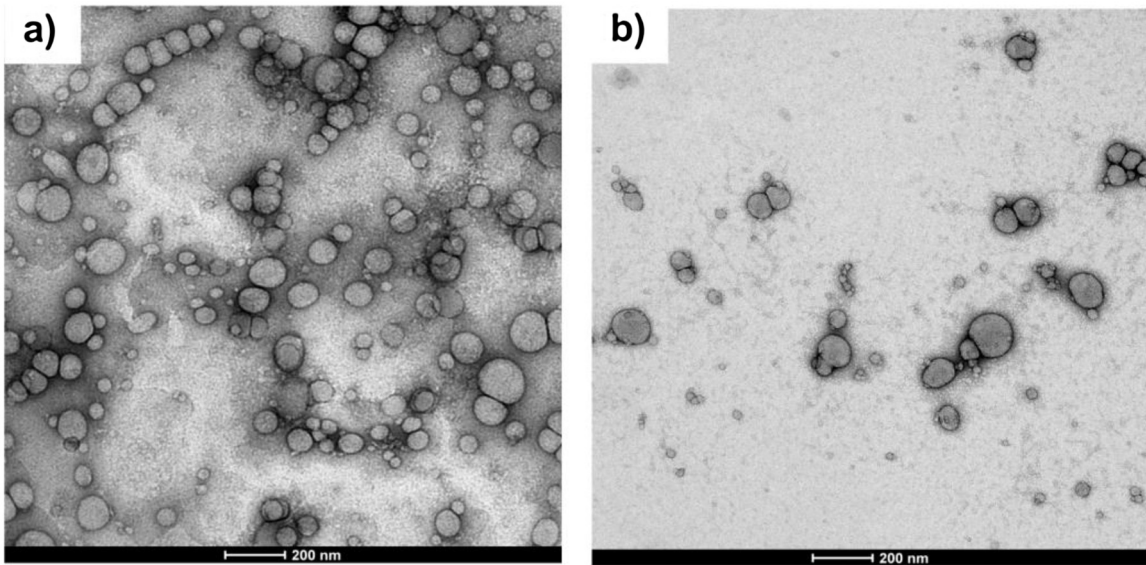


**Fig. 4.** TEM images of the hybrid latexes (a)  $MC_0$  and (b)  $MC_{40}$ .

some hard domains of casein [31]. Moreover, Nikiforow et al. [32], suggested that charged particles are an important source of self-stratification on films. Charged particles strongly resist enrichment at the film/air interface because of their mutual repulsion. Consequently, the top surface of latex blends would be richer in less charged nanoparticles. In the present study, the final pH of the hybrid latex  $MC_0$  resulted much higher than the isoelectric point of the protein (pH ~4) and therefore casein exhibits a neat charge, which favors its migration towards the bottom of the film. These mechanisms may also explain the higher CA observed for the films formed when employing native casein, as it will be shown in the following section.

On the other hand, when compatibility is increased by using MC, higher amount of casein is chemically anchored to the polymer particle, and protein migration is restricted. Fig. 5b-d shows that when the system compatibility is progressively increased by augmenting the pendants methacrylic groups in MC, CGE ranged from 20% to 76%, and the film surface exhibits a more homogeneous distribution of its components. It can further be seen that the inner part of the  $MC_{40}$  material (Fig. 6b) presents a similar phase distribution

to that observed on the surface, also indicating a high degree of uniformity throughout the film. Both kind of images (surface and cross-sectional cut) reveal that the core-shell particle morphology is conserved.

These results demonstrate that the use of MC is an excellent alternative to improve phase compatibility of the film, obtaining more homogeneous materials at the nanoscale level.

Notice that the film morphology observed in Figs. 5 and 6 reveals that particle coalescence mainly occurred in the casein phase wherein water is a good solvent and acts as plasticizer, favoring the film formation. Moreover, it is worth mentioning that free-monomer in acrylic latexes (up to 26%) also could act as a plasticizer of the polymer particles during film formation, thus helping to the particle coalescence.

### 3.4. Properties of the hybrid materials

Table 3 summarizes the results of  $T_{d,max}$ , CA and anti-blocking rate for the hybrid films obtained from casein with different degree of methacrylation. Notice that when reducing the fraction

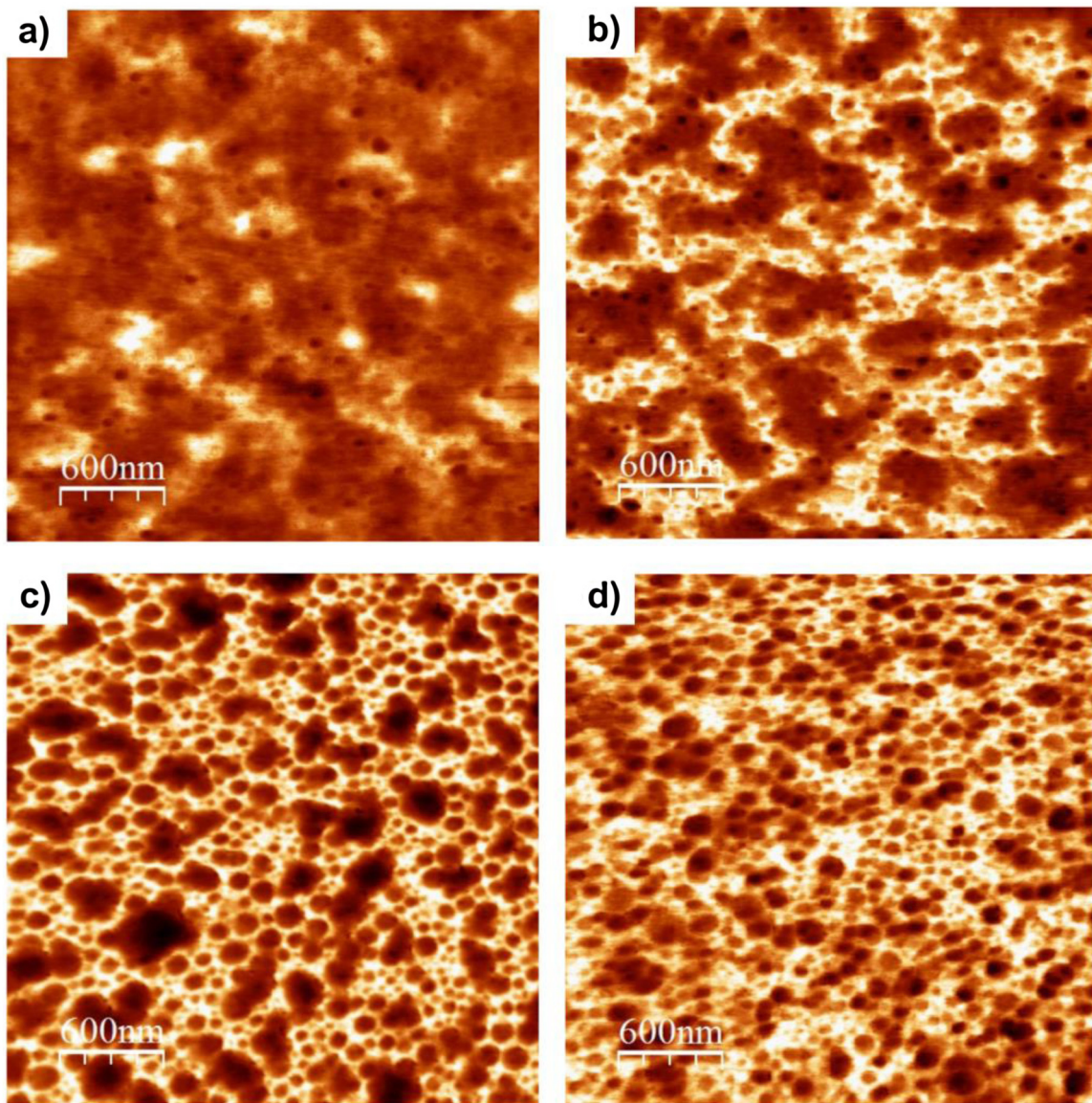


**Fig. 5.** AFM ( $3\text{ }\mu\text{m} \times 3\text{ }\mu\text{m}$ ) phase images of films surfaces of hybrid materials MC<sub>0</sub> (a); MC<sub>2</sub> (b); MC<sub>10</sub> (c); and MC<sub>40</sub> (d).

**Table 3**  
Final values of  $T_{d,\text{max}}$ , CA and anti-blocking rate for the hybrid films.

Film	$T_{d,\text{max}}$ (°C)	CA (°)	Anti-blocking Rate
MC <sub>0</sub>	402.0	81.6	8
MC <sub>2</sub>	393.0	80.1	8
MC <sub>10</sub>	419.0	76.1	9
MC <sub>20</sub>	420.0	72.2	10
MC <sub>40</sub>	417.0	70.9	10

of ungrafted casein by incorporating MC (i.e., a higher fraction of casein with acrylic polymer linked onto its backbone),  $T_{d,\text{max}}$  of the hybrid materials is notably increased.

Also, the films CA that characterize their surface were reduced when increasing the acrylic/casein compatibility (from 81.6° for MC<sub>0</sub>, to 70.9° for MC<sub>40</sub>). This observation is in agreement with the surface morphologies of the films above presented, where the compatibility increment in the hybrid nanoparticles leads to higher casein content on the film surface, due to limitations in the molecular mobility of this component during the drying process. Therefore, the higher concentration of protein (the more hydrophilic component) on the surface resulted in a decrease of CA.

One of the biggest challenges in coating technology is the production of binders able to simultaneously attain smooth film formation at room temperature (low minimum film formation temperature, MFFT) and high blocking resistance, which is a key performance requirement for water-based architectural coatings. As it is known, conventional waterborne binders have poor block resistance. However in a recent work[20], we have demonstrated that the addition of casein to acrylic formulations could improve the blocking resistance, since the protein is a glassy component that confers hardness to the film bulk and reduces the tack adhesion energy [33,34]. Table 3 shows that formulations with MC, containing 10 or more vinyl double bonds, present higher blocking resistance values than film with native casein. For high degree of functionality (MC<sub>20</sub> and MC<sub>40</sub>), completely non-blocking films were obtained. This behavior is directly related to the film morphology previously discussed where its surface is enriched by the hard casein, contributing to improve the blocking properties. Also, the presence of high grafted polymer fractions in the films, as a consequence of the addition of double bonds onto casein chain (Table 2), restricts the molecular mobility of soft acrylic chains and

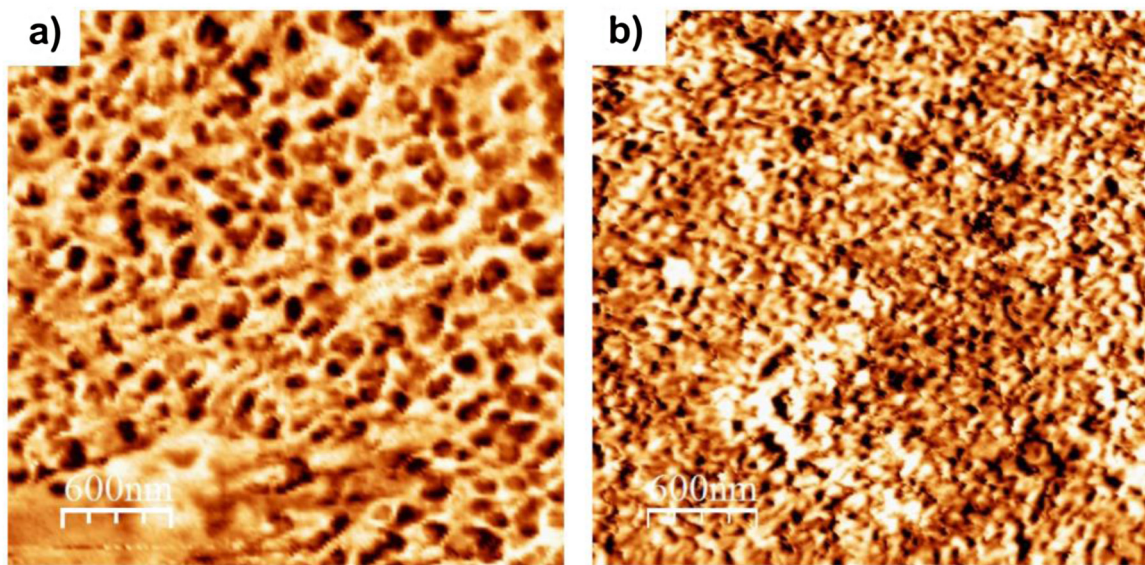


**Fig. 6.** AFM ( $3 \mu\text{m} \times 3 \mu\text{m}$ ) stiffness images of cross-section cuts of hybrid materials MC<sub>0</sub> (a) and MC<sub>40</sub> (b).

**Table 4**

Mechanical behavior for hybrid materials obtained from MC with different degree of methacrylation.

Film	Young's module (MPa)	Tensile strength (MPa)	Elongation at break (%)	Hardness (N)
MC <sub>0</sub>	$37.0 \pm 3.0$	$5.4 \pm 0.3$	$396 \pm 39$	$435 \pm 22.2$
MC <sub>2</sub>	$49.0 \pm 2.7$	$6.5 \pm 0.3$	$423 \pm 9$	$428 \pm 21.5$
MC <sub>10</sub>	$32.9 \pm 3.1$	$8.0 \pm 0.3$	$657 \pm 34$	$319 \pm 38.8$
MC <sub>20</sub>	$18.6 \pm 1.8$	$8.0 \pm 0.5$	$575 \pm 38$	$258 \pm 30.0$
MC <sub>40</sub>	$7.6 \pm 0.5$	$7.7 \pm 0.4$	$398 \pm 27$	$144 \pm 23.7$

reduces the adhesion of the materials [35], and therefore improves the blocking resistance.

The current position of water-based paints in the world market is 60% of the architectural paints, and it continuously increases due to the innovative chemistries of high performance. Despite their numerous advantages such as easy water cleaning, low odour and low environmental impact, one of the remaining problems of water-based systems is the too short open time compared to the solvent-based systems. The open-time of a paint is defined as the period of time during which a painter can make corrections to the freshly applied wet paint film without leaving brush marks [36,37]. Water-based decorative paints typically 'close' around 5–10 min, while decorative solvent-based paints in 30–40 min [38]. To gain more open-time, an efficient approach is the addition of water soluble organic compounds, such as glycol derivatives, to control the rheology and delay the evaporation of the water [37]. However, this approach increases the total VOC in the formulation.

The here synthesized hybrid latexes present open times ranging from 20 to 30 min, close to that of a solvent-based paints, which implies a great advantage for this polymer/casein system. The higher open time of the hybrid latexes in relation to conventional water-based paints could be attributed to the presence of casein, an amphiphilic compound which acts as a surface active agent keeping water inside the film for longer periods of time [39].

The mechanical test results of the hybrid materials are shown in Table 4. It can be observed that the mechanical behavior of the films resulted strongly dependent on the degree of compatibility. Thus, the increase of CGE from 20% (for native casein) to 76% (for MC<sub>40</sub>), produced a decrease in the Young module and hardness of the films. This behavior is attributed to the reduction of the ungrafted casein into the films, which acts as a reinforcing agent

**Table 5**

Water and solvent resistance of hybrid films obtained from MC with different degree of methacrylation.

Film	Water Resistance		MEK Resistance	
	A <sub>W</sub> (%)	WL <sub>W</sub> (%)	A <sub>MEK</sub> (%)	WL <sub>MEK</sub> (%)
MC <sub>0</sub>	–	100	70.6	23.8
MC <sub>2</sub>	–	100	126.9	11.6
MC <sub>10</sub>	360.5	10.6	72.7	8.1
MC <sub>20</sub>	231.3	9.5	58.5	7.7
MC <sub>40</sub>	135.0	11.1	44.7	7.6

of the polymeric matrix [20]. In other words, when hard casein is highly grafted with the rubbery polymer, the resulting hybrid material is softer due to the increase of compatibility. It could be expected that the reduction of the free casein content in films, also would be accompanied by both a decrease in the tensile strength and an increase in the elongation ability of the materials. However, note that the tensile strength of the films does not follow the expected trend, increasing from 5.4 MPa for MC<sub>0</sub> to 8.0 MPa in the case of MC<sub>10</sub>, without additional variation for higher casein methacrylation degrees. In addition, the elongation of the materials was improved as increasing the degree of casein functionality until MC<sub>10</sub>, but further increases (MC<sub>20</sub> and MC<sub>40</sub>), caused a degradation of this property. These results clearly suggest that, besides the effect of reducing the free casein content, there is another phenomenon which oppositely contributes to the mechanical behavior of the films. Based on the IF and CGE results, the higher cross-linking density of the material when the degree of casein methacrylation is increased, contributes to generate cross-linked networks inside films, also affecting both tensile strength and elongation capability.

### 3.5. Water and solvent resistance

From Table 5 it can be observed that, hybrid films obtained with native casein disintegrated after water immersion, likely because of the low compatibility achieved where a high amount of ungrafted protein is present in the film. Under these conditions, the ungrafted casein is transferred to the water phase and this migration process disintegrates the films.

The incorporation of MC considerably improved the resistance to water immersion, resisting the films 7 days of immersion without presenting damage and notably reducing the percentage of

**Table 6**

Biodegradation of acrylic/casein films obtained from MC with different degree of methacrylation.

Film	Weight loss after 7 days (%)	Weight loss after 14 days (%)
MC <sub>0</sub>	29.6	29.7
MC <sub>2</sub>	20.5	24.4
MC <sub>10</sub>	25.6	26.8
MC <sub>20</sub>	21.5	23.9
MC <sub>40</sub>	23.7	25.4

absorbed water ( $A_W$ ). When using MC with 10 or more vinyl functionalities an outstanding performance was reached, with immersion times larger than 7 days and final weight loss ( $WL_W$ ) of around 10%. Also note that  $A_W$  decreased with the degree of compatibilization as a consequence of both the increase in the cross-linking density of films and the reduction of the amount of NH<sub>2</sub> groups in the biomaterial structure, by using MC with higher degree of methacrylation, that limit the water swelling. Based on these results, the strategy of casein methacrylation with GMA successfully overcame the deficient water resistance of the films, expanding the possibilities of the latexes for their use as waterborne binders in coatings.

On the other hand, Table 5 also shows the results of MEK resistance for the hybrid materials. The incorporation of a hydrophilic component as casein, improved the organic solvent barrier, giving as result that all hybrid films resisted 7 days of immersion in MEK, with respect to pure acrylic film which was completely swollen in such solvent ( $WL_{MEK} = 100\%$ ). Notice that the absorbed solvent mass ( $A_{MEK}$ ) and weight loss of the films ( $WL_{MEK}$ ) were considerably reduced when increasing the number of methacrylic groups incorporated per casein, probably due to the higher degree of cross-linking achieved in those cases.

### 3.6. Biodegradation

The results of soil biodegradation are presented in Table 6, as the weight lost by the films ( $W_{loss}$ ) after 7 and 14 days. As it can be observed, the incorporation of casein improved the biodegradability of the films, by significantly increasing  $W_{loss}$  of the hybrid materials in relation to pure acrylic polymer (from 0.34% for the acrylic film up to around 25%, for the hybrid materials). Furthermore, since protein is the responsible of the degradable character of hybrid films, it could be supposed that an increase in the number of grafted acrylic chains onto casein, should lead to less degradable materials. The biodegradation results of Table 6 show that film containing native casein present a  $W_{loss}$  of around 30%, slightly higher than those films containing MC (close to 25%). Note that the degree of methacrylation of MC does not significantly affect the degradation capability of the hybrid films, obtaining values of  $W_{loss}$  (after 14 days) in agreement with the biomaterial content. The small difference in  $W_{loss}$  observed from Table 6 is also evident in the SEM images of the biodegraded films. Fig. 7 compares photos of films before and after biodegradation and the SEM images of biodegraded materials. Despite of biodegraded films do not present macroscopic differences (Fig. 7a), some dissimilarity are microscopically observed (Fig. 7b). It could be noted that the lost mass in film with native casein covers big areas and presents a deep degradation related with the great amount of ungrafted casein and its phase migration. On the other hand, when using MC<sub>40</sub> a more uniform degradation is observed with small domains of lost mass. These results are in agreement with the observed morphologies of Figs. 5 and 6.

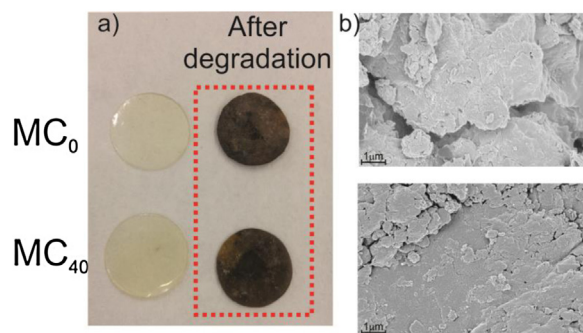


Fig. 7. Biodegradation of MC<sub>0</sub> and MC<sub>40</sub> films. Photos of films before and after biodegradation (a) and SEM images of biodegraded films (b).

## 4. Conclusions

The coatings application of waterborne acrylic/casein latexes demands an adequate balance between the properties of the biopolymer (hard and hydrophilic) with those of the synthetic polymer (soft and hydrophobic). Materials synthesized with neat casein present low degree of compatibility, which restrict their application as high performance film-forming products. A method to successfully control acrylic/casein compatibility extent, based on using methacrylated caseins (MC) with varied degree of methacrylation in an emulsifier-free emulsion polymerization of acrylic monomers, was presented. Hybrid latexes obtained with this proposal exhibited reduced fractions of ungrafted components, while the bio-component was compatibilized by means of a high number of grafted acrylic chains onto its backbone. As result, latexes synthesized with MC presented enhanced film properties, resulting in a material with a more homogeneous phase distribution. It importantly expands the possibilities of using these latexes as waterborne binders in coatings, where good key performance parameters of the films, as thermal decomposition, blocking resistance, mechanical behavior, open-time and resistance to water and solvents, were reached.

## Acknowledgements

The financial support received from CONICET, ANPCyT, the Secretary of Science, Technology and Innovation of Santa Fe State, and the Secretary of University Policies from the Education Ministry (all of Argentina) is gratefully acknowledged. We are also grateful to the Physics of Surfaces and Interfaces Laboratory (IFIS Litoral, UNL-CONICET) for the use of their SPM equipment and to Dr. Santiago Vaillard (INTEC) for his help with the NMR measurements.

## References

- [1] J.J. Bozell, Clean 36 (2008) 641–647.
- [2] C.K. Williams, M.A. Hillmyer, Polym. Rev. 48 (2008) 1–10.
- [3] M. Eissen, J.O. Metzger, E. Schmidt, U. Schneidewind, Angew. Chem. Int. Ed. 41 (2002) 414–436.
- [4] G.W. Huber, S. Iborra, A. Corma, Chem. Rev. 106 (2006) 4044–4098.
- [5] H.K. Salzberg, L.E. Georgevits, R.M. Karapetoff Cobb, Casein in paper coating, in: L.H. Silvernail, W.M. Bain (Eds.), Synthetic and Protein Adhesives for Paper Coating, Technical Association of the Pulp and Paper Industry, New York, 1961, pp. 103–166.
- [6] S. Ednessjord, Natural glues, in: S. Ednessjord (Ed.), Adhesives Technology Handbook, William Andrew, Norwich, 2008, pp. 95–97.
- [7] Y. Liu, Y. Zhang, Z. Liu, K. Deng, Eur. Polym. J. 38 (2002) 1619–1625.
- [8] H.A. Currie, S.V. Patwardhan, C.C. Perry, P. Roach, N.J. Shirtcliffe, Natural and artificial hybrid biomaterials, in: G. Kickelbick (Ed.), Hybrid Materials: Synthesis, Characterization and Applications, Wiley-VCH Verlag GmbH & Co., Weinheim, 2007, pp. 255–299.
- [9] Q. Xu, J. Ma, J. Zhou, Y. Wang, J. Zhang, Chem. Eng. J. 228 (2013) 281–289.
- [10] J. Ma, Q. Xu, J. Zhou, D. Gao, J. Zhang, L. Chen, Prog. Org. Coat. 76 (2013) 1346–1355.

- [11] X.H. Qiang, Q. Xue, H. Zhang, Z. Yan, M. Li, W. Xu, Y.J. Wang, *J. Coat. Technol. Res.* 11 (2014) 923–931.
- [12] Q. Xu, F. Zhang, J. Ma, T. Chen, J. Zhou, D. Simion, G. Carmen, *Prog. Org. Coat.* 88 (2015) 1–7.
- [13] F. Zhang, J. Ma, Q. Xu, J. Zhou, D. Simion, G. Carmen, *Colloids Surf. A* 484 (2015) 329–335.
- [14] Q. Xu, Q. Fan, J. Ma, Z. Yan, *Prog. Org. Coat.* 99 (2016) 223–229.
- [15] P. Li, J.H. Liu, Q. Wang, C. Wu, *Macromol. Symp.* 151 (2000) 605–610.
- [16] Y. Liu, J. Li, L. Yang, Z. Shi, J. Macromol. Sci. Chem. 41 (2004) 305–316.
- [17] P. Li, J. Zhu, P. Sunintaboon, F.W. Harris, *Langmuir* 18 (2002) 8641–8646.
- [18] J. Zhu, P. Li, J. Polym. Sci. A: Polym. Chem. 41 (2003) 3346–3353.
- [19] M.L. Picchio, R.J. Minari, V.D.G. González, M.C.G. Passeggi (Jr.), J.R. Vega, M.J. Barandiaran, L.M. Gugliotta, *Macromol. Symp.* 344 (2014) 76–85.
- [20] M.L. Picchio, M.C.G. Passeggi Jr., M.J. Barandiaran, L.M. Gugliotta, R.J. Minari, *Prog. Org. Coat.* 88 (2015) 8–16.
- [21] M.L. Picchio, R.J. Minari, V.D.G. Gonzalez, M.J. Barandiaran, L.M. Gugliotta, *J. App. Polym. Sci.* 132 (2015), <http://dx.doi.org/10.1002/app.42421>.
- [22] L. Shechter, J. Wynstra, P. Kurkij, *Ind. Eng. Chem.* 48 (1956) 94–97.
- [23] Y. Liu, R. Gou, *Biophys. Chem.* 136 (2008) 67–73.
- [24] K. Wiberg, *Angew. Chem. Int. Ed. Engl.* 25 (1986) 312–322.
- [25] F.J. Morales, C. Romero, S. Jiménez-Pérez, *J. Food Prot.* 58 (1995) 310–315.
- [26] M.S. Vigo, L.S. Malec, R.G. Gomez, R.A. Llosa, *Food Chem.* 44 (1992) 363.
- [27] V.J.K. Svedas, I.J. Galaev, I.L. Borisov, I.V. Berezin, *Anal. Biochem.* 44 (1992) 363–365.
- [28] D.J. McMahon, B.S.J. Oommen, *J. Dairy Sci.* 91 (2008) 1709–1721.
- [29] I. Horcas, R. Fernández, J.M. Gómez-Rodríguez, J. Colchero, J. Gómez-Herrero, A.M. Baro, *Rev. Sci. Instrum.* 78 (2007) 013705.
- [30] J.S. Nunes, S.J. Bohórquez, M. Meeuwisse, D. Mestach, J.M. Asua, *Prog. Org. Coat.* 77 (2014) 1523–1530.
- [31] J.L. Keddie, A.F. Routh, *Fundamentals of Latex Film Formation: Processes and Properties*, Springer, Dordrecht, The Netherlands, 2010.
- [32] I. Nikiforow, J. Adams, A.M. König, A. Langhoff, K. Pohl, A. Turshatov, D. Johannsmann, *Langmuir* 26 (2010) 13162–13167.
- [33] S.T. Eckersley, B.J. Helmer, *J. Coat. Technol.* 69 (1997) 97–107.
- [34] R.S. Gurney, D. Dupin, J.S. Nunes, K. Ouzineb, E. Siband, J.M. Asua, S.P. Armes, J.L. Keddie, *ACS Appl. Mater. Interfaces* 4 (2012) 5442–5452.
- [35] W. Wenjun, M. Anderson, J. Schneider, *JCT Coat. Technol.* 6 (2009) 22–26.
- [36] S. Kiil, *Prog. Org. Coat.* 57 (2006) 236–250.
- [37] A. Overbeek, F. Bückmann, E. Martin, P. Steenwinkel, T. Annable, *Prog. Org. Coat.* 48 (2003) 125–139.
- [38] A. Brun, H. Dihang, L. Brunel, *Prog. Org. Coat.* 61 (2008) 181–191.
- [39] J. Maldonado-Valderrama, A. Martín-Rodríguez, M.A. Cabrerizo-Vischez, M.J. Galvez Ruiz, *Interfacial phenomena underlying the behavior of foams and emulsion*, in: R. Hidalgo-Álvarez (Ed.), *Structure and Functional Properties of Colloidal Systems*, Taylor and Francis Group, Norwich, 2009, pp. 219–233.